Int. J. Heat Mass Transfer. Vol. 32, No. 1, pp. 87–94, 1989
Printed in Great Britain

0017–9310/89 $3.00 + 0.00

Natural convection in an inclined square enclosure with a partition attached to its cold wall

RAMÓN L. FREDERICK
Departamento de Ingeniería Mecánica, Universidad de Chile, Casilla 2777, Santiago, Chile

(*Received* 22 *December* 1987 *and in final form* 3 *June* 1988)

Abstract—Natural convection in an air-filled, differentially heated, inclined square cavity, with a diathermal partition on its cold wall is numerically studied, at Rayleigh numbers of 10^3–10^5. The partition causes convection suppression, and heat transfer reductions of up to 47% relative to the undivided cavity at the same Rayleigh number. Heat transfer reduction depends on Rayleigh number, partition length and inclination. For long partitions, transition to bicellular flow occurs. At high Rayleigh numbers the heat transfer reduction is affected by secondary buoyancy forces, generated by the partition. Applications to the reduction of solar collector heat losses are discussed.

INTRODUCTION

NATURAL convection in cavities of complex geometry has attracted the interest of several researchers. This paper describes the effect of adding a baffle to the cold wall of an air-filled, differentially heated, inclined enclosure. The study is motivated by the growing interest to find means to improve the insulating properties of fluid layers. This situation has a wide range of applications, especially related to the reduction of heat losses from flat plate solar collectors.

Most works about cavities of complex geometry deal with partitions fitted to insulated walls [1–3], and they usually show that velocities, stream functions and Nusselt numbers are reduced with respect to their values for undivided cavities at the same Rayleigh number. Cavities with baffles on their active walls have been less studied. Bejan [4] considers a vertical cavity filled with a fluid-saturated porous medium, and with a partial diathermal divider attached to the cold wall. For Darcy–Rayleigh numbers of 50–1000, the average Nusselt number is lower than its value for the undivided cavity in most cases. However, in the conduction regime, a slight increase in $\overline{Nu}$ is observed in divided, tall cavities. The use of adiabatic dividers increases the heat transfer. Therefore, heat transfer depends strongly on the thermal behavior of the partition.

Oosthuizen and Paul [5] studied an air-filled rectangular cavity with a horizontal plate on the cold wall. They found increases in heat transfer when the plate was adiabatic or perfectly conducting. Shakerin *et al.* [6], considered an enclosure with discrete roughness elements on the cold wall. In laminar flow, very small increases in heat transfer are obtained even if the roughness elements are perfectly conducting. Both works are in the context of the heat transfer augmentation. Works on external natural convection on surfaces attached to active vertical walls are very scarce. Sparrow and Chrysler [7] gave experimental results for a short horizontal cylinder attached to a vertical plate of the same temperature. Due to the interaction with the plate boundary layer, the cylinder Nusselt number is reduced by 10–20% relative to that for a long horizontal cylinder.

From these results, it is reasonable to expect that when a partition of very small thickness (δ) and very low thermal conductivity is attached to one of the active walls, a reduction of heat transfer through the cavity with respect to the case of the undivided cavity will be obtained. If the length of the partition (d) is such that $d \gg \delta$, the partition can be taken as diathermal across its thickness, with a big thermal resistance along d. It will be shown that the effect of a diathermal divider fitted to the cold wall of an inclined, air-filled cavity can be a reduction in heat transfer. The ranges of variables of interest in this work are similar to those currently found in flat plate solar collectors [8]: air gap thicknesses from 1 to 2.5 cm, temperature differences up to perhaps 80°C, and Rayleigh numbers (based on the air gap thickness) of 10^3–10^5. The angles of inclination from the horizontal are often equal to the latitude. Aspect ratios (A) in solar collectors are generally between 20 and 200. As a first step, main consideration is here given to square enclosures. Some results for an aspect ratio of 2.0 are also given. Interest is focused on the effects of Rayleigh number, inclination angle and partition length on flow and heat transfer.

FORMULATION

The physical situation is shown in Fig. 1. The hot and cold walls, at temperatures T_2 and T_1, respectively, make an angle ϕ with the horizontal. The other two walls are insulated. Midway between the insulated walls, and parallel to them, a partial partition of length d and thickness δ is fitted to the cold wall. The dimensionless governing equations, in terms of the stream

NOMENCLATURE

A	aspect ratio, H/L
d	partition length [m]
g	gravitational acceleration [m s^{-2}]
H	cavity height [m]
L	cavity width [m]
n	inward normal to the wall
Nu	local Nusselt number on hot wall
$\overline{Nu}$	average Nusselt number on hot wall
Pr	Prandtl number of air
Ra	Rayleigh number, $g\beta(T_2-T_1)L^3/\nu\alpha$
T	temperature
T_m	average fluid temperature, $(T_2+T_1)/2$
T_2, T_1	hot and cold wall temperatures
u	dimensionless velocity in x-direction
v	dimensionless velocity in y-direction
x, y	dimensionless coordinates.

Greek symbols

α	thermal diffusivity of air [m^2 s^{-1}]
β	thermal expansion coefficient of air [K^{-1}]
δ	partition thickness [m]
θ	dimensionless temperature, $(T-T_m)/(T_2-T_1)$
θ_{ab}	average baffle temperature
ν	kinematic viscosity of air [m^2 s^{-1}]
τ	dimensionless vorticity
ϕ	angle of inclination
ψ	dimensionless stream function
ψ_{max}	maximum dimensionless stream function.

Reference quantities

L	for coordinates
α/L	for velocities
α/L^2	for vorticity
α	for stream function.

function and vorticity in permanent, conservative form, for two-dimensional laminar flow of an incompressible Boussinesq fluid are

$$\frac{\partial(u\tau)}{\partial x}+\frac{\partial(v\tau)}{\partial y}= -Ra\,Pr\left(\frac{\partial\theta}{\partial x}\cos\phi+\frac{\partial\theta}{\partial y}\sin\phi\right)+Pr\,\nabla^2\tau \quad (1)$$

$$\frac{\partial(u\theta)}{\partial x}+\frac{\partial(v\theta)}{\partial y}=\nabla^2\theta \quad (2)$$

$$\tau=-\nabla^2\psi \quad (3)$$

$$u=\partial\psi/\partial y;\quad v=-\partial\psi/\partial x. \quad (4)$$

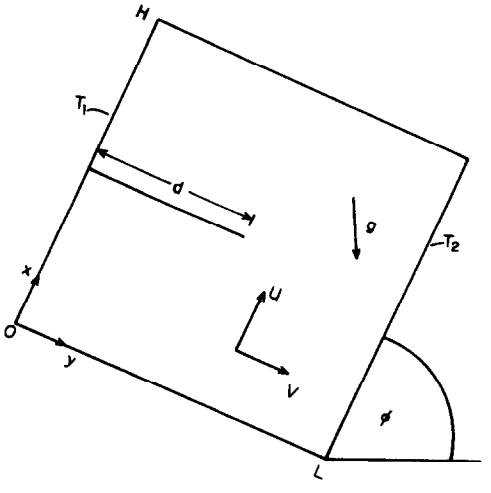

FIG. 1. Physical situation and coordinates.

The use of the Boussinesq approximation yields adequate heat transfer results for $(T_2-T_1)/T_1 \leqslant 0.2$ in square cavities [9]. In solar collectors, with glass temperatures of about 300 K, the Boussinesq approximation would not be valid at $(T_2-T_1) > 60°C$. Such temperature differences are obtained using selective absorbers. As in most cases the temperature difference will not exceed 60°C, the Boussinesq approximation will be considered valid for this study.

The no-slip boundary conditions for the enclosure walls and the partition are $u = v = \psi = 0$. Vorticity conditions on all solid walls are

$$\tau=-\partial^2\psi/\partial n^2. \quad (5)$$

Wall vorticity takes different values at the upper and lower faces of the divider. The temperatures on the hot and cold walls are $\theta = 0.5$ and -0.5, respectively. On the insulated walls, $\partial\theta/\partial x = 0$. In the field of application of this study, the partition should be very thin ($d \gg \delta$), and transparent to solar radiation, in order not to interfere with solar energy collection. Appropriate materials for it would be glass or plastic, which have relatively low thermal conductivities. The partition is assumed to interfere only with fluid motion and not with conduction across the thickness.

A Prandtl number of 0.71 will be used. The angles of inclination (ϕ) will be varied from 45° to 90°, in order to ensure that two-dimensional flow is obtained. Rayleigh numbers of 10^3–10^5 will be considered.

NUMERICAL METHOD

Discretized forms of equations (1)–(3) were solved by a finite difference over-relaxation procedure. Uniform square meshes of 41×41 and 51×51 points

with mesh sizes of 0.025 and 0.020 were used. As the baffle is very thin, it is taken as a single line of mesh points, so the vorticity at the partition is doubly valued. For the partition tip, the discontinuous vorticity formulation recommended by Roache [10] is used.

The mesh size was selected as a compromise between accuracy and speed of computation in the range of Rayleigh numbers to be covered. de Vahl Davis [11] shows that a step size of 0.025, used in conjunction with a second-order method, gives enough accuracy in the undivided square cavity problem (test problem) at $Ra = 10^3$ and 10^4. At a Rayleigh number of 10^5, the error in the average wall Nusselt number using this mesh size is 1.22% as compared with his benchmark solution, whereas at $Ra = 10^6$ the error is 5.14%. As the upper limit in Ra in this study is 10^5, a mesh size of 0.025 is acceptable. However, for Rayleigh numbers above 7×10^4 a mesh size of 0.020 was used. No significant differences were found between results obtained with both mesh sizes at lower Rayleigh numbers. Predictions of average hot wall Nusselt numbers for the test problem were compared with values given by de Vahl Davis for the 41×41 mesh. The relative errors found were 1.52, 1.56 and 2.45% at Rayleigh numbers of 10^3, 10^4 and 10^5, respectively. As a further check on the numerical results, average Nusselt numbers at the hot and cold walls were compared, and they differed by less than 0.5% in all computer runs.

RESULTS AND DISCUSSION

Results for the vertical cavity will be described first, with reference to Figs. 2 and 3. Figure 2(a) shows the streamlines at $Ra = 10^4$ with a partition of dimensionless length $d/L = 0.5$. Without partition ($d/L = 0$), the usual circulation pattern, in which the fluid rotates counterclockwise around the midpoint (which is also the point of maximum stream function), is obtained. With a partition, the point of maximum stream function is displaced upwards and sidewards Table 1 shows the flow effects of the partition for a sample of the results. At $Ra = 10^4$ in the test problem, the maximum values of velocity v near the top and bottom walls of the cavity are equal and of opposite signs. The divider causes asymmetry in the velocity distribution: the maximum value of v towards the cold wall exceeds the maximum towards the hot one. Circulation and velocities are reduced with respect to those of the test problem at the same Rayleigh number, the reduction being more significant for longer partitions. The overall effect of the divider is a suppression of convection.

Flow variables increase with Ra (Fig. 3(a)). The maximum stream function for $d/L = 0.5$ was 98% of its value for the test problem at $Ra = 10^5$. The corresponding percentage at $Ra = 10^4$ was only 40%. This shows that, although with a different flow pattern, the flow variables tend to recover the levels of the test problem as Ra increases.

Isotherms for the above situations are shown in Figs. 2(b) and 3(b). In the test problem, at $Ra = 10^4$, a boundary layer regime exists. The presence of the divider deeply alters the temperature field: at $Ra = 10^4$, the nearly horizontal isotherms of the test problem are replaced by nearly vertical ones, specially around the divider. This behavior is observed also at higher Rayleigh numbers, although as Ra increases, the temperature stratification tends to reappear. (See, e.g. the isotherms for $\theta = -0.3, -0.2, -0.1, 0.2$ and 0.3 in Fig. 3(b).) In all cases, the isotherms show that the heat flow through the partition is upwards. Significant horizontal temperature gradients are established at different levels of the vertical midplane (Fig. 2(b)). Thermal boundary layers are thickened, and the temperature gradients at the hot wall are reduced from their values for the test problem at the same Ra. This implies that a reduction in the heat transfer through the cavity occurs. Figure 4(a) shows

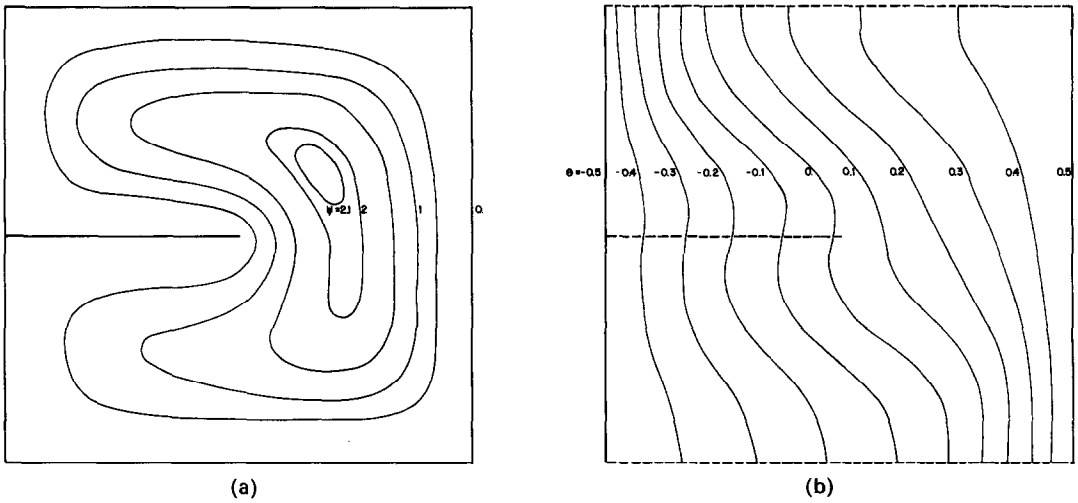

(a) (b)

FIG. 2. Isograms at $Ra = 10^4$, $d/L = 0.5$, $\phi = 90°$: (a) stream function contours; (b) isotherms.

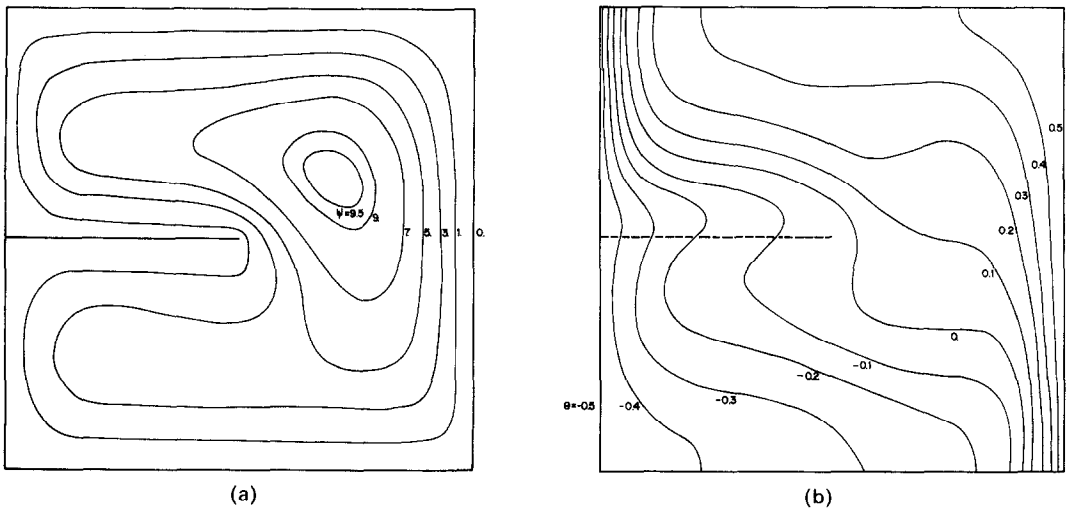

FIG. 3. Isograms at $Ra = 10^5$, $d/L = 0.5$, $\phi = 90°$: (a) stream function contours; (b) isotherms.

Table 1. Effects of partition on flow variables

Ra	ϕ	d/L	u_{max}	v_{max}	ψ_{max}
10^4	90	0	19.5	16.2	5.10
		0.25	17.1; −18.5	12.4; −13.8	4.07
		0.5	11.7; −13.2	9.22; −10.3	2.14
10^4	45	0	24.8	24.4	7.45
		0.25	21.1; −23.9	15.8; −18.3	5.31
		0.5	12.3; −14.0	10.1; −13.0	2.53
		0.75	7.51	9.93	1.68

the variation of the average hot wall Nusselt number with Ra and d/L. It is evident that the partition has an insulating effect. The percentage by which $\overline{Nu}$ is reduced with respect to the test problem at the same Ra is given in Table 2. At $d/L = 0.5$, reductions of over 30% in $\overline{Nu}$ are observed in the range of Ra from 2500 to 30 000, with a maximum reduction at $Ra = 8000$. The reduction is smaller at $d/L = 0.25$. As Ra increases above the value which gives maximum heat transfer reduction, the boundary layers formed on all solid walls grow progressively thinner, and the

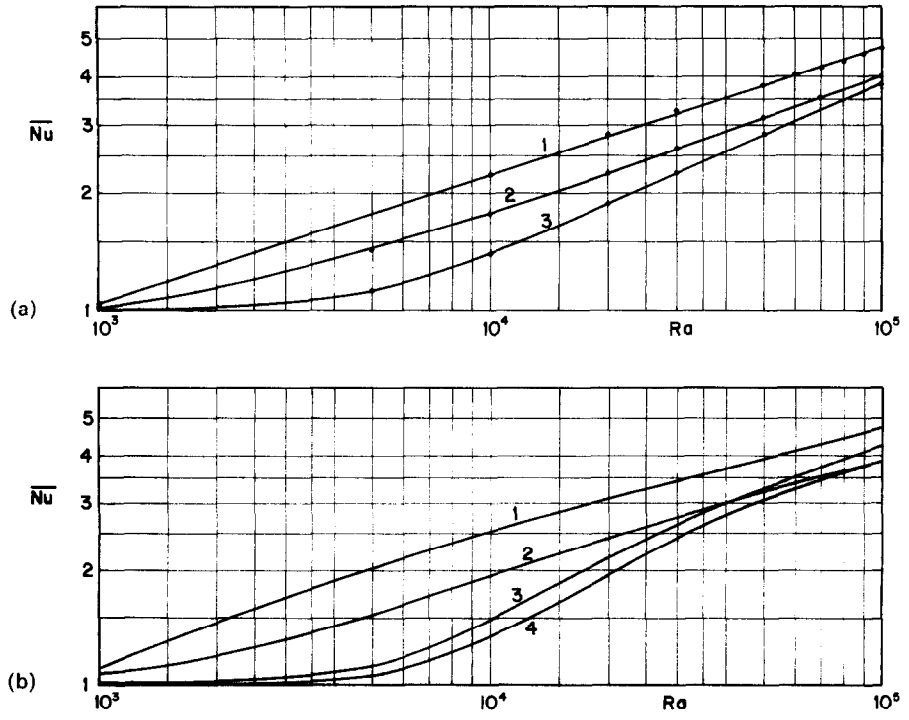

FIG. 4. Variation of average Nusselt number with Ra and d/L. Curves 1, $d/L = 0$; Curves 2, $d/L = 0.25$; Curves 3, $d/L = 0.5$; Curve 4, $d/L = 0.75$. (a) $\phi = 90°$; (b) $\phi = 45°$.

Table 2. Average Nusselt number reduction at $\phi = 90°$, percentage

$Ra \times 10^{-3}$	1	5	10	20	30	50	70	100
$d/L = 0.25$	7.83	20.85	21.37	19.89	19.78	17.47	15.22	13.79
$d/L = 0.50$	11.41	36.83	38.40	33.14	29.77	24.02	20.15	17.48

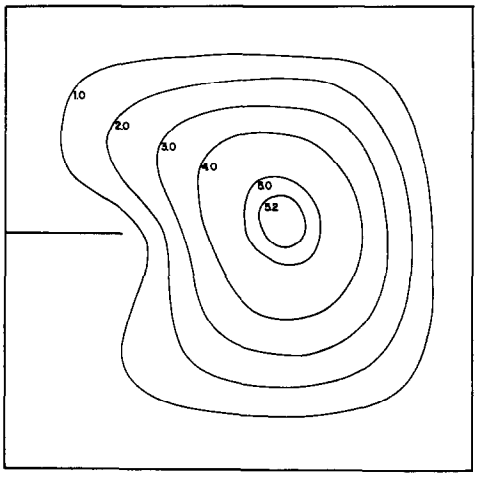

FIG. 5. Isograms at $Ra = 10^4$, $d/L = 0.25$, $\phi = 45°$. Stream function contours.

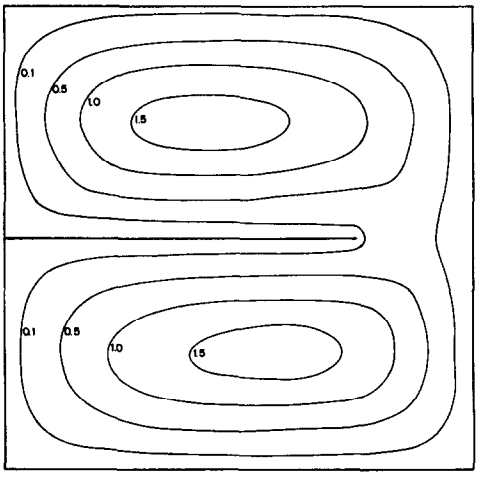

FIG. 6. Stream function contours at $Ra = 10^4$, $d/L = 0.75$, $\phi = 45°$.

velocity and temperature profiles near the hot wall tend to resemble those observed without partition. Therefore, the progressive diminution of the insulating effect at high Ra agrees with the trends observed in stream functions and isotherms. It is also seen that the slope of the $\overline{Nu}$–Ra curve above $Ra = 20\,000$ is higher in the case of $d/L = 0.5$ than at 0.25.

Results for inclined cavities are now described. The full range of Rayleigh numbers was explored for $\phi = 45°$. Fewer results were obtained for $\phi = 60°$ and 75°. A comparison of results for the test problem with 45° and 90° of inclination (Table 1), shows that convection is more intense in the former case. The boundary layer character of the flow is reduced due to the inclination. The effect of the divider is shown in Figs. 5 and 6 for $Ra = 10^4$. An increase in partition length increases the asymmetry of the flow pattern. At $d/L = 0.75$ a second vortex appears in the lower half of the cavity. The exchange of fluid between the top and bottom halves of the enclosure is made up by a thin layer circulating adjacent to the bounding walls of the cavity and around the divider. As in the case of $\phi = 90°$, the isotherms tend to become parallel to the active walls near the obstacle. Heat transfer reduction is also observed at $\phi = 45°$ (Table 3). At Rayleigh numbers below 20 000, the reduction is slightly higher than in vertical cavities. Figure 4(b) shows the dependence of $\overline{Nu}$ on Ra and on d/L at a 45° inclination. The heat transfer decreases with an increase in d/L at Rayleigh numbers up to 40 000. Above this limit, the average Nusselt number in a cavity with long partition ($d/L = 0.5$) exceeds the value for a cavity with short partition ($d/L = 0.25$). This occurrence is maintained as Ra increases, and it happens also at $\phi = 60°$, although starting from a Rayleigh number of 5×10^4. In addition, the Nusselt number for $d/L = 0.75$ exceeds the one for $d/L = 0.25$ at 45° of inclination from a Rayleigh number of about 8×10^4 on.

This behavior is explained by the local Nusselt number profiles on the hot wall (Fig. 7). At $Ra = 10^4$, the values of Nu are higher for $d/L = 0.25$ than for other partition lengths along most of the hot wall. Local Nusselt numbers for $d/L = 0.75$ are the smallest, except in a region above $x = 0.6$. At $Ra = 7 \times 10^4$, the behavior is more complex: at $d/L = 0.25$ and 0.5, Nu has a maximum near the lowest end of the hot wall. However, for $d/L = 0.75$, two local maxima occur. This is because the flow behaves as a two-cell flow. Part of the fluid cooled by the cold wall is diverted by the partition towards the hot one, producing a local increase in Nusselt number from $x = 0.5$ upwards.

With shorter partitions, a second maximum in Nu was not observed. However, the local Nusselt numbers in the lower part of the hot wall were significantly higher at $d/L = 0.5$ than at 0.25. In spite of this, the absolute maximum in stream function was 11.5 in the former case, and 14.7 in the latter, showing that the overall circulation was stronger with the short partition, as expected. The behavior of local Nusselt number can be explained in terms of local circulation in the lower half of the cavity. A comparison of stream function values at some representative points, at $Ra = 7 \times 10^4$ (Table 4) shows that the circulation in the right-hand half of the lower left quarter of the cavity is stronger when a longer partition is attached to the cold wall. Negative u-velocities near the cold wall show local 'maximum' values of -18.8 and -31.1 when short and long baffles are present, respectively. Thus, the fluid is cooled more effectively by the

Table 3. Average Nusselt number reduction at $\phi = 45°$, percentage

$Ra \times 10^{-3}$	1	5	10	20	30	50	70	100
$d/L = 0.25$	2.28	24.78	23.16	21.27	20.34	19.53	19.06	18.60
$d/L = 0.50$	8.30	43.59	40.67	29.10	22.58	15.99	12.84	11.03
$d/L = 0.75$	8.31	46.10	47.50	36.67	29.15	22.25	19.33	—

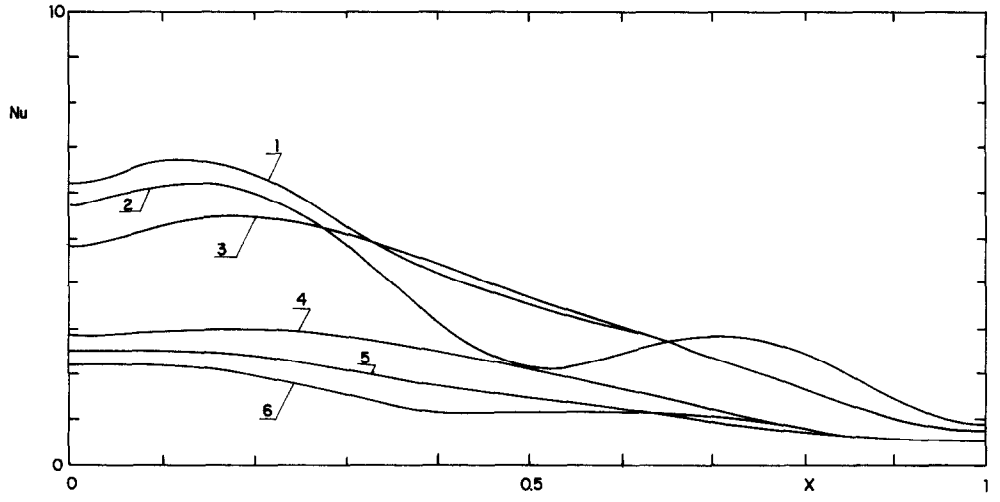

FIG. 7. Local Nusselt number distribution on hot wall, $\phi = 45°$. Curves 1–3, $Ra = 70\,000$; Curves 4–6, $Ra = 10\,000$; Curves 1 and 5, $d/L = 0.5$; Curves 3 and 4, $d/L = 0.25$; Curves 2 and 6, $d/L = 0.75$.

Table 4. Circulation conditions in the lower left quarter of the cavity. Stream function values at specified positions, $Ra = 7 \times 10^4$, $\phi = 45°$

	$d/L = 0.50$			$d/L = 0.25$		
	x					
y	0.125	0.250	0.375	0.125	0.250	0.375
0.125	2.28	3.15	1.49	1.68	1.53	0.37
0.250	3.92	5.26	2.31	2.72	2.37	0.72
0.375	3.90	5.49	2.06	3.65	5.47	6.57
0.500	3.52	4.98	1.49	4.74	9.20	12.10
θ_{ab}		−0.175			−0.304	

cold wall in the latter case. If a cooler fluid approaches the hot wall, a higher Nusselt number will be obtained on it. It is also seen (Table 4) that the average baffle temperature is higher at $d/L = 0.5$ than at 0.25. In the former case, even the temperature average for the half of the baffle adjacent to the cold wall (-0.289) exceeds the average for the whole of the short baffle. The divider can thus be seen as a secondary source of buoyancy forces, the effect of which is noticeable at high Rayleigh numbers when the cavity is inclined, i.e. when the buoyancy forces acting on the fluid below the divider have a non-zero component parallel to it. This effect shows a tendency for the flow to become a two-cell flow. This tendency manifests itself at higher values of d/L.

The influence of the main variables on the average heat transfer is summarized as follows: at given values of Ra and d/L, higher values of $\overline{Nu}$ are found in inclined cavities than in vertical ones. At low Ra, the average Nusselt number decreases with increases in partition length. The same trend is found at higher Ra only in vertical cavities. In inclined cavities the heat transfer shows a maximum at about $d/L = 0.5$. At a fixed Ra, the rate of decrease of heat transfer with d/L is higher in the range of low values of this parameter. In a cavity with 45° inclination, the percentage heat transfer reduction at $d/L = 0.25$ is nearly constant in the range of Ra from 10^4 to 10^5 (approximately 23–19%). That is, the $\overline{Nu}$–Ra curve remains nearly parallel to that for the undivided cavity. This length of partition will therefore be more convenient than $d/L = 0.5$, in which the heat transfer reduction becomes progressively smaller as Ra increases.

Some results were obtained for a cavity with a partition on the hot wall. They show that, even at $\phi = 90°$, the average Nusselt numbers for a long partition exceed those for a short one from a certain value of Ra on. This is also related with the secondary buoyancy forces generated by the partition. When the baffle is hot, these forces provoke a local increase of circulation above it, with a corresponding increase in the heat transfer rate.

A few trial runs were made for a rectangular cavity of aspect ratio $A = 2.0$, with a divider of $d/L = 0.5$, at $\phi = 45°$. A bicellular flow pattern is established (Fig. 8(a)), and the maximum stream function (8.27) is greatly increased from its value for unit aspect ratio at the same Rayleigh numbers and dimensionless partition lengths. The isotherms (Fig. 8(b)) show a local distortion of the temperature field, located mainly around the divider. In the zones defined by $x < 0.5$

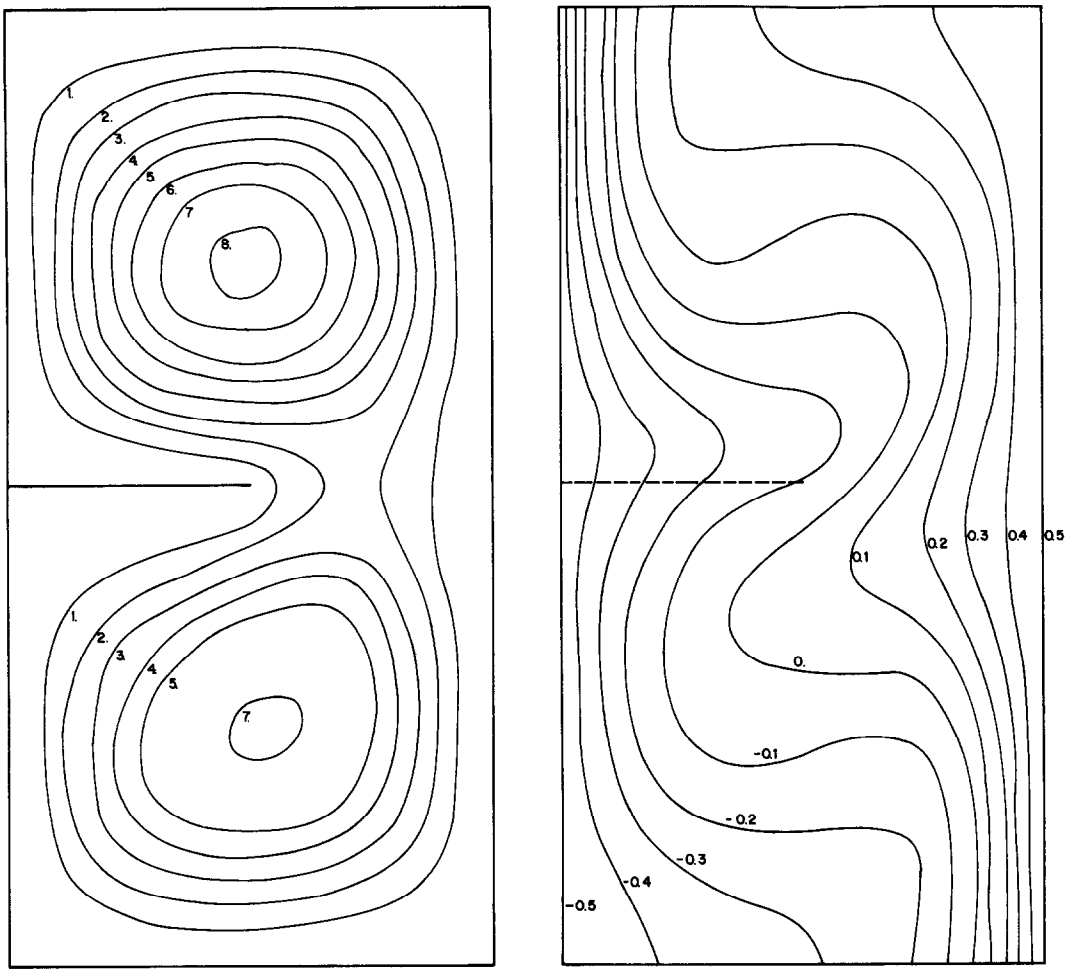

FIG. 8. Isograms at $Ra = 10^4$, $A = 2$, $d/L = 0.5$, $\phi = 45°$: (a) stream function contours; (b) isotherms.

and $x > 1.5$, the isotherms do not differ greatly from those obtained without partition, confirming that the effect of the partition is a local one. Two maxima in local Nusselt number occur. A reduction in the average heat transfer was also noticed in this case, although limited to 12.1% at Rayleigh numbers of 5×10^3 and 10^4.

CONCLUSIONS

The presence of a diathermal partition on the cold wall of a square, air-filled, differentially heated enclosure caused decreases of up to 47% in the heat transfer with respect to the test case at the same Rayleigh number. The percentage heat transfer reduction, which was small at $Ra = 10^3$, had a maximum between 7×10^3 and 10^4 and then decreased progressively. This reduction was due to a partial suppression of convection. At low Ra, the boundary layers were thicker than those for the test case. As Ra grew, boundary layers got progressively thinner, and the effects of the partition on the temperature field became more and more localized around the partition. This was confirmed by the results obtained in enclosures of aspect ratio 2.0. When the partition length was considerable, secondary circulations appeared, which tended to produce increases in heat transfer.

The percentage heat transfer reduction grows with partition length for all the angles of inclination investigated up to Rayleigh numbers of about 4×10^4, where the effect of convection suppression is dominant. At higher Rayleigh numbers, in inclined cavities, the relatively hot wall of the divider generates secondary buoyancy forces which increase with the partition length, thereby increasing the circulation below the divider and the average heat transfer rate. As this is related with the temperature distribution in the partition, it would be interesting to investigate the effect of conduction along the divider on the average heat transfer rate.

The effects described could be useful for reducing convective losses in solar collectors if they were observed also in high aspect ratio, rectangular cavities. As the insulating effect was related to a local distortion of the temperature field, it can be anticipated that multiple partitions would be required in rectangular

cavities to reach the levels of heat transfer reduction reported here for square cavities. As the use of long partitions will probably stimulate the appearance of multiple vortexes and secondary buoyancy forces, short partitions (of d/L about 0.25) are likely to be appropriate for obtaining significant heat transfer reductions in rectangular cavities. If the divider thickness and thermal conductivity are considerable, Nusselt numbers are likely to exceed the values obtained in this work for a given Rayleigh number.

Acknowledgements—Funds provided by DIB (Departamento de Investigación y Bibliotecas, Universidad de Chile), Project I-2624, are gratefully acknowledged. I would also like to thank the reviewers for their valuable suggestions.

REFERENCES

1. S. Acharya and C. H. Tsang, Natural convection in a fully partitioned, inclined enclosure, *Numer. Heat Transfer* **8,** 407–428 (1985).
2. L. C. Chang, J. R. Lloyd and K. T. Yang, A finite difference study of natural convection in complex enclosures, *Proc. 7th Int. Heat Transfer Conf.*, Munich, F.R.G., Vol. 2, pp. 183–188 (1982).
3. N. N. Lin and A. Bejan, Natural convection in a partially divided enclosure, *Int. J. Heat Mass Transfer* **26,** 1867–1878 (1983).
4. A. Bejan, Natural convection heat transfer in a porous layer with internal flow obstructions, *Int. J. Heat Mass Transfer* **26,** 815–822 (1983).
5. P. H. Oosthuizen and J. T. Paul, Free convection heat transfer in a cavity fitted with a horizontal plate on the cold wall. In *Advances in Enhanced Heat Transfer—1985* (Edited by S. M. Shenkman *et al.*), ASME HTD Vol. 43 (1985).
6. S. Shakerin, M. Bohn and R. I. Loehrke, Natural convection in an enclosure with discrete roughness elements on a vertical heated wall, *Proc. 8th Int. Heat Transfer Conf.*, San Francisco, U.S.A., Vol. 4, pp. 1519–1525 (1986).
7. E. M. Sparrow and G. M. Chrysler, Natural convection heat transfer coefficients for a short horizontal cylinder attached to a vertical plate, *ASME J. Heat Transfer* **103,** 630–637 (1981).
8. H. Buchberg, I. Catton and D. K. Edwards, Natural convection in enclosed spaces—a review of application to solar energy collection, *ASME J. Heat Transfer* **98,** 182–188 (1976).
9. Z. Y. Zhong, K. T. Yang and J. R. Lloyd, Variable property effects in laminar natural convection in a square enclosure, *ASME J. Heat Transfer* **107,** 133–138 (1985).
10. P. J. Roache, *Computational Fluid Dynamics*, pp. 169 ff. Hermosa, Albuquerque, New Mexico (1976).
11. G. de Vahl Davis, Natural convection of air in a square cavity. A benchmark numerical solution, *Int. J. Numer. Meth. Fluids* **3,** 249–264 (1983).

CONVECTION NATURELLE DANS UNE ENCEINTE CARREE INCLINEE, AVEC UNE CLOISON ATTACHEE A LA PAROI FROIDE

Résumé—On étudie numériquement la convection naturelle dans une cavité carrée inclinée, remplie d'air, chauffée différentiellement, avec une cloison sur la paroi froide, pour des nombres de Rayleigh de 10^3–10^5. La séparation provoque la suppression de la convection et une réduction du transfert thermique allant jusqu'à 47% du cas de la cavité sans cloison. Cette situation dépend du nombre de Reynolds, de la longueur de la séparation et de l'inclinaison. Pour des longues cloisons, apparait la transition à l'écoulement bicellulaire. Aux grands nombres de Reynolds, la réduction du transfert thermique est influencée par des forces secondaires de flottement dues à la cloison. On discute des applications de cette réduction aux pertes thermiques d'un collecteur solaire.

NATÜRLICHE KONVEKTION IN EINEM GENEIGTEN HOHLRAUM VON QUADRATISCHEM QUERSCHNITT MIT EINER UNTERTEILUNG

Zusammenfassung—Die natürliche Konvektion in einem luftgefüllten, abschnittsweise beheizten, geneigten quadratischen Hohlraum mit einer wärmedurchlässigen Trennwand zur kalten Wand wird numerisch für *Ra*-Zahlen von 10^3 bis 10^5 untersucht. Die Trennwand unterdrückt die Konvektion und verringert den Wärmestrom bis zu 47%—bezogen auf den nicht unterteilten Hohlraum bei gleicher *Ra*-Zahl. Die Verringerung des Wärmestroms ist abhängig von der *Ra*-Zahl, von der Länge der Zwischenwand und von der Neigung. Bei langen Zwischenwänden erfolgt ein Übergang zu zwei Konvektionswalzen. Bei großen *Ra*-Zahlen wird die Verringerung des Wärmestroms von sekundären Auftriebskräften beeinflußt, die durch die Trennwand hervorgerufen werden. Anwendungsmöglichkeiten zur Verringerung der Wärmeverluste von Solarkollektoren werden diskutiert.

ЕСТЕСТВЕННАЯ КОНВЕКЦИЯ В НАКЛОННОЙ ЗАМКНУТОЙ ПОЛОСТИ КВАДРАТНОГО СЕЧЕНИЯ С ПЕРЕГОРОДКОЙ, ПРИКРЕПЛЕННОЙ К ЕЕ ХОЛОДНОЙ СТЕНКЕ

Аннотация—Численно изучается естественная конвекция в заполненной воздухом неоднородно нагретой наклонной полости квадратного сечения с теплопроводящей перегородкой, укрепленной на ее холодной стенке, в диапазоне чисел Рэлея от 10^3 до 10^5. Перегородка препятствует развитию конвекции и уменьшает теплоперенос до 47% по сравнению с полостью без перегородки при тех же числах Рэлея. Уменьшение теплопереноса зависит от числа Рэлея, длины и угла наклона перегородки. В случае длинных перегородок течение становится двухъячеистым. При больших числах Рэлея вторичные подъемные силы, вызванные перегородкой, также способствуют уменьшению теплопереноса. Обсуждается использование данной модели для отыскания путей снижения теплопотерь солнечного коллектора.